Research on the image rotation of the polar coordinates infrared inertial stable platform with four reflected mirrors

Qiu Zhaowen, Song Liquan, Zhang Bingtong

(Tianjin Jinhang Institute of Technical Physics, Tianjin 300308, China)

Abstract: The angle of the image rotation was studied which was caused by the movements of two frames of polar coordinates direct stable platform and indirect stable platform with four reflected mirrors. The result shows that both the movements of pitching-frame and rolling-frame cause the image rotation. The angle of image rotation of indirect stable platform which was caused by rolling-frames increased when the abaxial angle increased. When the abaxial angle was small, the angle of image rotation of indirect stable platform which was caused by rolling-frames was also small. The angle of image rotation of direct platform was direct ratio with the tangent of the angle of rolling-frame and was inverse ratio with the cosine of the angle of pitching-frame. The result of simulation shows that the angle of image rotation of indirect stable platform with four reflected mirrors was smaller than the direct stable platform and has lower influence on imaging.

Key words: polar coordinates inertial stable platform; image rotation; four reflected mirrors; direct stable platform; indirect stable platform

CLC number: TJ765 **Document code:** A **DOI:** 10.3788/IRLA201746.1217004

四反射镜结构极坐标红外惯性稳像平台像旋研究

邱兆文,宋利权,张炳通

(天津津航技术物理研究所,天津 300308)

摘 要: 针对极坐标式直接稳像平台结构和间接稳像平台的四反射镜成像光路结构, 推导其两框架运动所引起的像旋角度。结果表明俯仰框和滚转框的运动均会引起像旋。四反射镜间接稳像结构像旋随着离轴角增大,滚转框运动所引起的像旋角度也逐渐增加,在小离轴角时,滚转所引起的像旋也较小。直接稳像结构像旋角度与滚转框架角的正切值成正比,与俯仰框架角的余弦值成反比。仿真结果表明,四反射镜结构像旋比直接稳像结构的要小,对成像质量影响小。

关键词: 极坐标惯性稳像平台; 像旋; 四反射镜; 直接稳像平台; 间接稳像平台

收稿日期: 2017-04-10; **修订日期:** 2017-05-20

作者简介: 邱兆文(1987-),男,工程师,主要从事红外光电导引系统研究、随动控制系统方面的研究。Email:qmiracle@163.com

0 Introduction

As science developed, traditional aerocrafts could not meet the needs of modernization. In order to adapt the needs, the new aerocrafts should have higher flexibility and the ability of launching with larger abaxial angle and the guiding system should have large field of view, small volume and light weight. All these features are restricted by the structure of frames of stable platform. We can obtain the large field of view by using the polar coordinates stable platform whose rolling–platform can roll from 0° to 360° and pitching–platform can move from –90° to 90°. Therefore, its field of view can cover the fore–semisphere. It′s the perfect choice of new aerocraft. Until now, American and European have developed their own polar coordinates stable platform, and have used on the aerocraft successfully. The polar coordinates stable platform make a good performance in practice[1–3].

1 Choice of the benchmark

Now polar coordinates infrared stable platform include two kinds of structures which are direct stable platform and indirect stable platform shown in Fig.1 and Fig.2.

Judging whether the image is rotating we should choose a benchmark as reference. In this paper, we choose the pitching–frame coordinate of the direct platform with yaw–pitch frames as the benchmark. It′s the virtual pitch coordinate of polar coordinates inertial stable platform. Its definition

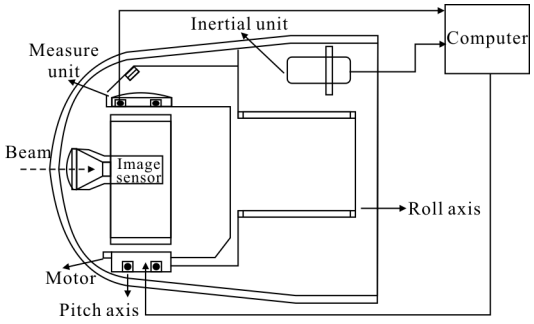

Fig.1 Direct stable platform

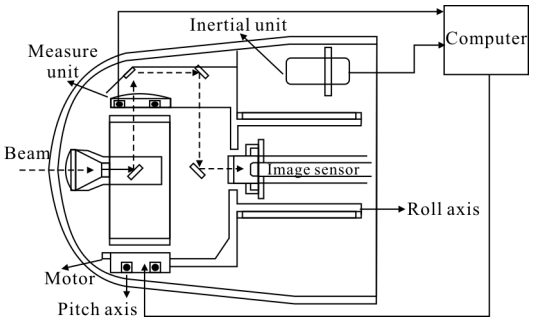

Fig.2 Indirect stable platform with four reflected mirrors

and relationship with polar coordinates structure are shown in reference [1].

There is a rolling angle θ_{GD} between the virtual pitch coordinate and the pitching–frame coordinate of the polar coordinates stable platform. This angle has a relationship with the rolling–frame angle γ_r and the pitching–frame angle ϑ_p shown in Eq.(1).

$$\tan\theta_{GD}=\sin\gamma_r/(\cos\gamma_r\cos\vartheta_p) \quad (1)$$

When the rolling angle is equal to zero, θ_{GD}=0°.

We can see from its definition, θ_{GD} is the angle of image rotation of the direct stable platform of polar coordinates.

2 Calculation of the angle of image rotation of the structure with four reflected mirrors

In Fig.3, L_0–L_4 are the vectors of the middle incidence beam and reflected beams of four reflected mirrors. N_1–N_4 are the normal unit vectors of four reflected mirrors.

As shown in Fig.3, because the reflected mirror is fixed on the pitching–frame, the coordinates of its normal vector N_1 in pitching–frame coordinate are:

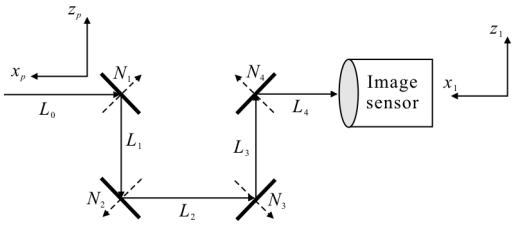

Fig.3 Lighting track structure with four reflected mirrors

$$N_1=\left[-\frac{\sqrt{2}}{2}\quad 0\quad \frac{\sqrt{2}}{2}\right]^{\mathrm{T}} \tag{2}$$

Reflected mirrors 2, 3, 4 are fixed on the rolling-frame, so the coordinates of their normal vectors N_2、N_3、N_4 in rolling-frame coordinate are:

$$N_2=\left[\frac{\sqrt{2}}{2}\quad 0\quad -\frac{\sqrt{2}}{2}\right]^{\mathrm{T}} \tag{3}$$

$$N_3=\left[-\frac{\sqrt{2}}{2}\quad 0\quad -\frac{\sqrt{2}}{2}\right]^{\mathrm{T}} \tag{4}$$

$$N_4=\left[\frac{\sqrt{2}}{2}\quad 0\quad \frac{\sqrt{2}}{2}\right]^{\mathrm{T}} \tag{5}$$

The coordinate transform matrix which expresses the change from incidence beam to reflected beam is:

$$L_{i\to r}=\begin{bmatrix}1-2N_x^2 & -2N_xN_y & -2N_xN_z\\ -2N_yN_x & -2N_y^2 & -2N_yN_z\\ -2N_zN_x & -2N_zN_y & 1-2N_z^2\end{bmatrix} \tag{6}$$

So substituting Eqs.(2)-(5) into Eq.(6) we can obtain all the transform matrixes:

The transform matrix of reflected mirror 1 in pitching coordinate system is:

$$L_{1p}=\begin{bmatrix}0 & 0 & 1\\ 0 & 1 & 0\\ 1 & 0 & 0\end{bmatrix} \tag{7}$$

The transform matrixes of reflected mirror 2, 3, 4 in pitching coordinate system are:

$$L_{2r}=\begin{bmatrix}0 & 0 & 1\\ 0 & 1 & 0\\ 1 & 0 & 0\end{bmatrix} \tag{8}$$

$$L_{3r}=\begin{bmatrix}0 & 0 & -1\\ 0 & 1 & 0\\ -1 & 0 & 0\end{bmatrix} \tag{9}$$

$$L_{4r}=\begin{bmatrix}0 & 0 & -1\\ 0 & 1 & 0\\ -1 & 0 & 0\end{bmatrix} \tag{10}$$

Because reflected mirror 2, 3, 4 are fixed on the rolling-frame, we can combinate them in one matrix as:

$$L_{234r}=\begin{bmatrix}0 & 0 & 1\\ 0 & 1 & 0\\ 1 & 0 & 0\end{bmatrix} \tag{11}$$

In this paper we derive the angle of image rotation from object to image. So in virtual pitching coordinate system, a facultative beam is assumed as:

$$[x_0\quad y_0\quad z_0]^{\mathrm{T}} \tag{12}$$

The coordinates of the beam which is paralleling with lighting axis is:

$$[x_0\quad 0\quad 0]^{\mathrm{T}} \tag{13}$$

So the vector of difference is:

$$[0\quad y_0\quad z_0]^{\mathrm{T}} \tag{14}$$

The real angle of the object which is between the difference vector and the y axis of the virtual pitching coordinate system is:

$$\Delta=\arctan\left(\frac{z_0}{y_0}\right) \tag{15}$$

Because the transformation is linear, we can transform the difference vector into image as:

$$\begin{bmatrix}x_{\mathrm{image}}\\ y_{\mathrm{image}}\\ z_{\mathrm{image}}\end{bmatrix}=L^{\mathrm{T}}(\gamma_r)L_{432r}L^{\mathrm{T}}(\vartheta_p)L_{1p}L(\theta_{GD})\begin{bmatrix}0\\ y_0\\ z_0\end{bmatrix}=$$
$$\begin{bmatrix}y_0\cos(\gamma_r-\vartheta_p-\theta_{GD})-z_0\sin(\gamma_r-\vartheta_p-\theta_{GD})\\ y_0\sin(\gamma_r-\vartheta_p-\theta_{GD})+z_0\cos(\gamma_r-\vartheta_p-\theta_{GD})\end{bmatrix} \tag{16}$$

Where $L(\theta_{GD})$ is the transform matrix between virtual pitching coordinate system and pitching-frame coordinate system.

$L(\vartheta_p)$ is the transform matrix between pitching-frame coordinate system and rolling -frame coordinate system.

$L(\gamma_r)$ is the transform matrix between rolling-frame coordinate system and body coordinate system.

So the angle between the image of difference vector and the y axis of image sensor is:

$$\Delta'=\arctan\left(\frac{y_0\sin(\gamma_r-\vartheta_p-\theta_{GD})+z_0\cos(\gamma_r-\vartheta_p-\theta_{GD})}{y_0\cos(\gamma_r-\vartheta_p-\theta_{GD})-z_0\sin(\gamma_r-\vartheta_p-\theta_{GD})}\right)=$$
$$\arctan\left(\frac{\tan(\gamma_r-\vartheta_p-\theta_{GD})+\tan\Delta}{1-\mathrm{an}(\gamma_r-\vartheta_p-\theta_{GD})\tan\Delta}\right)=$$

$$\gamma_r-\vartheta_p-\theta_{GD}+\Delta \tag{17}$$

The angle of image rotation is:

$$\theta_{swing}=\gamma_r-\vartheta_p-\theta_{GD} \tag{18}$$

3 Simulation

Because the relationship between angle of image rotation and frame angles is not linear, some special angles are chosen for simulation, plot and observe curves. We choose angles as 0°, ±30°, ±70°, ±90° and observe curves of relationship between the angle of image rotation and rolling-frame angle as shown in Fig.4-Fig.10.

As we can see in these figures, in the condition of four reflected mirrors with the abaxial angle zero, the angle of image rotation is 0° when the rolling-frame rotates. As the abaxial angle increased, the angle of image rotation also increase when the rolling-frame rotates. When the abaxial angle is equal to 90°, the relationship between angle of image rotation and rolling angle is linear separately in positive and negative side. In the condition of direct stable structure, the angle of image rotation is always larger. Except for the condition that the abaxial angle is 90°, the angle of image rotation can reach the maximum value |±180°| when the rolling-frame rotates.

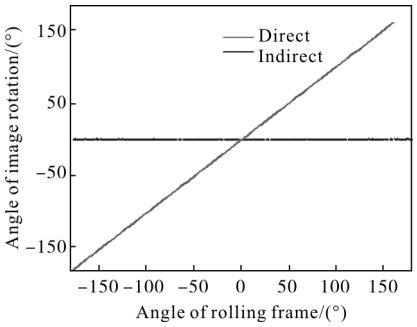

Fig.4 Pitching angle is 0°

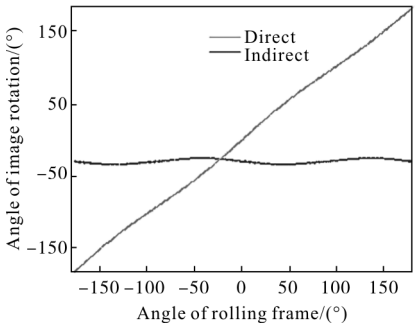

Fig.5 Pitching angle is 30°

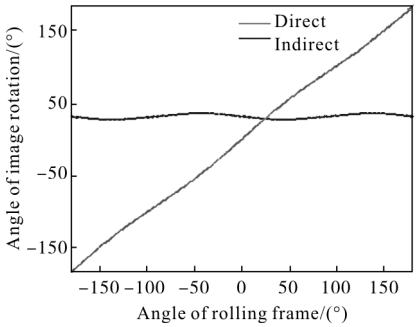

Fig.6 Pitching angle is −30°

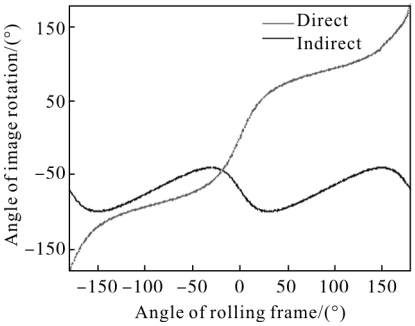

Fig.7 Pitching angle is 70°

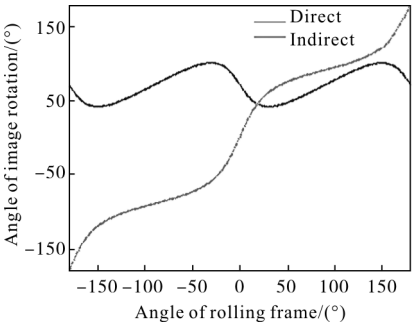

Fig.8 Pitching angle is −70°

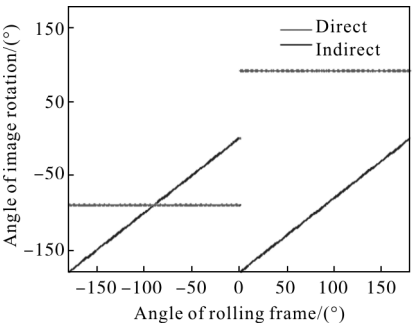

Fig.9 Pitching angle is 90°

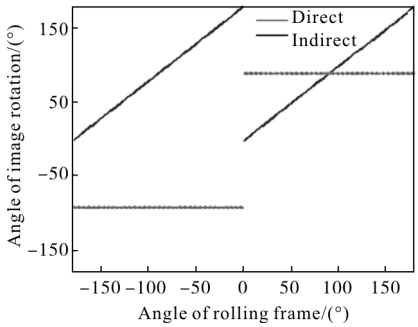

Fig.10 Pitching angle is −90°

4 Test with indirect stable platform

In order to prove the truth of the above equations, using the indirect stable platform of polar coordinates to test in the following conditions:

(1) The angle of pitching-frame is 0°, the angle of rolling-frame is 0°. The image took by indirect stable platform is shown in Fig.11.

From Fig.11 we can see the angle of image rotation is 0°, and equals to the result of Eq.(18).

Fig.11 Image on condition 1

(2) The angle of pitching-frame is 0°, the angle of rolling-frame is 40°. The image took by indirect stable platform is shown in Fig.12.

From the Fig.12 we can see the angle of image rotation is 0°, and equals to the result of Eq.(18). Also we can see that no matter what the angle of rolling-frame is, the angle is always 0° when the abaxial angle is 0°.

(3) The angle of pitching-frame is 30°, the angle of rolling-frame is 0°. The image took by indirect stable platform is shown in Fig.13.

Fig.12 Image on condition 2

Fig.13 Image on condition 3

From Fig.13 we can see the angle of image rotation is −30°, and equals to the result of Eq. (18).

(4) The angle of pitching-frame is 30°, the angle of rolling-frame is 40°. The image took by indirect stable platform is shown in Fig.14.

From Fig.14 we can see the angle of image rotation is −34.09°, and equals to the result of Eq.(18).

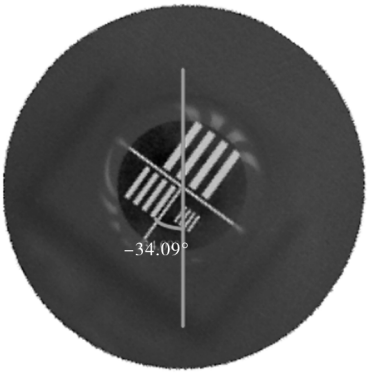

Fig.14 Image on condition 4

We also do a lot of tests in many different conditions, all the results equal to the results caculated by using Eq.(18). So the truth of Eq.(18) is proved.

5 Conclusion

The angle of image rotation of direct stable platform of polar coordinates caused by the rotation of rolling-frame is bigger. When the abaxial angle equals to 0°, the angle of image rotation equals to the angle of rolling-frame. In order to keep stabilization, the rotating speed is higher when the abaxial is closed to 0°. So the image of direct stable platform rotates violently and has a badly influence. The image rotation of indirect stable platform of polar coordinates caused by the rolling-frame when the abaxial angle closed to 0° is lower, so there is no influence on the image quality. When the abaxial angle is larger, the rolling-frame rotates slowly, the image rotation can be compensated by arithmetic, so there is also no influence on the image quality.

References:

[1] Qiu Zhaowen. Research on technology of control system of polar coordinates infrared inertial stable platform [D]. Tianjin: Tianjin Jinhang Institute of Technical Physics, 2013. (in Chinese)
邱兆文. 滚-仰式导引头控制系统技术研究 [D]. 天津: 天津津航技术物理研究所, 2013.

[2] Mu Xuezhen, Zhou Shuping, Zhao Guijin. Analysis and evaluation of new technology of AIM-9X's seeker[J]. ***Infrared and Laser Engineering***, 2006, 35(4): 392-400. (in Chinese)
穆学祯, 周树平, 赵桂瑾. AIM-9X 空空导弹位标器新技术分析和评价[J]. 红外与激光工程, 2006, 35(4): 392-400.

[3] Wang Zhiwei, Qi Zaikang, Wang Jiang. The tracking theory of roll-pitch seeker [J]. ***Infrared and Laser Engineering***, 2008, 37(2): 274-277. (in Chinese)
王志伟, 祁载康, 王江. 滚—仰式导引头跟踪原理[J].红外与激光工程, 2008, 37(2): 274-277.

[4] Qian Xingfang, Lin Ruixiong, Zhao Yanan. Missile Aero Dynamics [M]. Beijing: Beijing Institute of Technology Press, 2008. (in Chinese)
钱杏芳, 林瑞雄, 赵亚男. 导弹飞行力学 [M]. 北京: 北京理工大学出版社, 2008.

[5] Shi Shunxiang, Wang Xueen, Liu Jinsong. Physical Optics and Applied Optics [M]. Xi′an: Xidian University Press, 2008. (in Chinese)
石顺祥, 王学恩, 刘劲松. 物理光学与应用光学[M]. 西安: 西安电子科技大学出版社, 2008.

[6] Dong Xiaomeng, Zhang Ping. Modeling and simulation for two-axis polar coordinate frame stabilized platform [J]. ***Journal of Detection & Control***, 2008, 30: 36-39. (in Chinese)
董小萌, 张平. 极坐标两轴稳定平台的模型与分析 [J]. 探测与控制学报, 2008, 30: 36-39.

[7] Chen Yu, Zhao Yan, Zhang Tonghe, et al. Tracking principle and simulation for roll-pitch strap-down seeker[J]. ***Aero Weaponry***, 2010(5): 55-64. (in Chinese)
陈雨, 赵剡, 张同贺, 等.滚仰式捷联导引头跟踪原理与仿真[J]. 航空兵器, 2010(5): 55-64.

[8] Russell T Rudin. Srapdown stabilization for imaging seekers[C]//Annual Interceptor Technology Conference, 1993.